Spectroscopic Study of Ytterbium in Amorphous Silicon Nitride

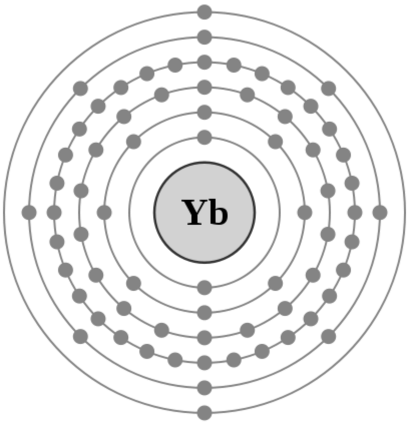

Thesis

submitted in partial fulfillment of the
requirements for the degree of

Bachelor of Science
in
Physics

Author : J.D. de Haan
Student ID : -
Supervisor : Dr. W. Löffler & Prof. Dr. D. Bouwmeester
2nd corrector : Dr.M.de Dood

Leiden, The Netherlands, July 11, 2017

Spectroscopic Study of Ytterbium in Amorphous Silicon Nitride

J.D. de Haan

Huygens-Kamerlingh Onnes Laboratory, Leiden University
P.O. Box 9500, 2300 RA Leiden, The Netherlands

July 11, 2017

Abstract

We investigated the largely unknown spectroscopic properties silicon nitride implanted with trivalent ytterbium ions. We found that annealing the implanted silicon nitride samples is essential to see the characteristic 980 nm Yb3+ peak in the photoluminescence spectrum. We also notice that the peak we measured in our spectrum is redshifted by 5 nm compared to other host materials, which is to be expected. Additionally, in our spectrum we measure a background that seems to be intrinsic to the host material or due to implantation damage, yet the exact cause is still to be found. We also estimated the density of excited Yb3+ in our samples which differed two orders of magnitude from our Yb implantation density which we deem a realistic result.

Keywords: *Ytterbium, Spectroscopy, Photoluminescence, Silicon nitride, Quantum memory*

Contents

CHAPTER 1
Introduction

1.1 Context and Motivation

Since 1980 there has been a need for quantum computing, and many small steps have been made to make this goal possible. The results of this project might be one of these small steps, though probably one of the smallest. One of the main functionalities a quantum computer needs is the ability to store quantum information. The problem of facilitating this storage has been tackled in multiple ways. One of the options is to store the quantum information of a photon into an atomic transition [1]. This quantum information can be, for instance, the superposition of the polarization or the spin state of the atomic transition. In figure 1.1 we see an example of the storage of a photon into an atomic transition. In this scheme there are two possibilities to store information, one is by storing an initial incoming photon by stimulated emission using a control laser pulse, shown in blue in the figure, to make the transition from an excited state $|e\rangle$ to a stable state $|s\rangle$. The other way would be to excite an electron from the ground state $|g\rangle$ to an excited state $|e\rangle$ using the control laser pulse which then by spontaneous emission emits a photon that puts it into a stable state $|s\rangle$. Later on this qubit can be read out by using the same laser or a different laser depending on the method. This laser excites the atom from the stable state to the excited state which then emits a photon that holds the information of this qubit. These methods can be achieved using a single atom, however multiple atoms can be used as well. Later on we will discuss which would be a better option for our study.

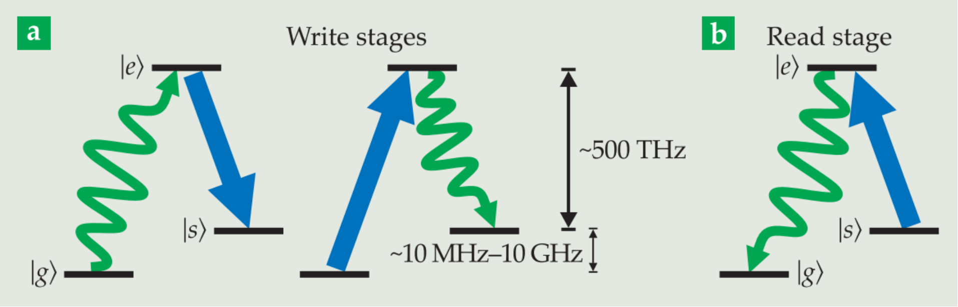

Figure 1.1: *An example of how quantum storage using atomic transitions would work. The frequency of these transitions shown next to the write stages are not relevant to our study. The image was originally created by M. Afzelius et al. [1]*

Another idea to make quantum storage possible using atomic transition is to use the Zeeman effect to split the ground state of the transition, as mentioned in a study done by P. Siyushev [2].
These methods of quantum storage do set a number of conditions upon the atomic transitions that can be used to efficiently and accurately store information. The atomic transition needs to be coherent, i.e. the photon that gets sent in has to have the same phase as the photon that comes out, and it needs to have a long lifetime so that the information can stay inside the transition for longer periods of time. The perfect candidate to make this work would be a single trapped atom, however this would be a very complex system. Moreover, for scalability a solid-state quantum memory, i.e. using multiple ions, would be more desirable.

Thus far attempts have been made to use rare earth elements, which seem to have these properties. However using these rare earth elements does come with a set of challenges. Since the transitions we are interested in have such a long lifetime, in the order of ms, there are not many photons to detect. A possible solution would be the use of microresonators [3, 4] to lower the lifetime of the transition as a result of Purcell enhancement [5]. The microresonator we are interested in is a waveguide that guides light traveling in a whispering gallery mode [6]. This requires the host material to have a high confinement of spatial modes. Attempts to create Yb doped mircoresonaters have as of yet only been made using silicon oxide as a host material.
Using amorphous silicon nitride as a host material would in theory lead to a high confinement of spatial modes, since it has a refractive index of $n_{SiN} \approx 2.0$ whereas silicon oxide has an refractive index of $n_{SiO} \approx 1.5$. Moreover, this makes the material a exemplary option for the use of waveguides and microresonators. Silicon nitride can be grown on top of silicon oxide and subsequently, a waveguide can be defined by lithography

and etching. Using amorphous silicon nitride makes this process easier since a crystalline structures makes it difficult to create smooth edges, since etching crystalline materials mostly is anisotropic. Though this also comes with disadvantages since it has been observed that amorphously structured materials show a tunneling effect: this means that atoms in this structure seem to tunnel between to positions with the same potential, as shown by W.Phillips [7] and A.Fleischmann et al. [8]. This in theory would cause the environment to be less stable, which would mean that more decoherence is induced in the Yb3+ transition. However, the details of tunneling systems in amorphous materials is still subject to active research.

1.2 Theory

1.2.1 Rare earth elements

Rare earth elements gain their properties from the fact that they have a partially filled 4f shell. Transitions within the 4f shell are parity forbidden due to the Laporte rule stating that in centrosymmetric molecules or atoms parity may not be conserved within an electronic transition. However the symmetry of an atom can be slightly disturbed by its environment, i.e. asymmetric vibrations, resulting in forbidden 4f-4f transitions, which have a very long lifetime.
Our main interests are focused upon trivalent ytterbium ions, since its 4f shell is missing only one electron and as a result has a relatively simple level scheme as can be seen in figure 1.1 below.

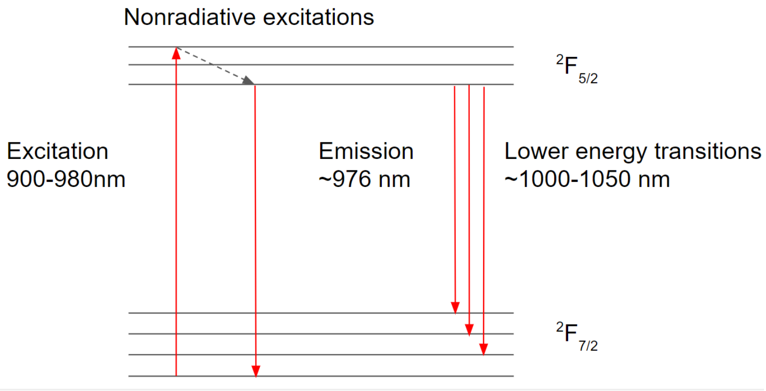

Figure 1.2: *Simplified level scheme of the Yb3+ 4f-4f transition we are interested in.*

This simple level scheme is partly the reason why they would be ideal, since other rare earth elements have a more complex level scheme. What helps in making the transition coherent is the fact that Yb3+ also has filled 5s and 5p shells. These shells, shield the transitions in 4f shell from the environment. This means environmental decoherence effects will be reduced.

1.2.2 Photoluminescence

The spectroscopic properties of ytterbium implanted in amorphous silicon nitride and the effects of annealing are largely unknown as of yet. To study these properties and effects we look upon the photoluminescence spectrum attributed to this material. Photoluminescence study can be done by exciting a material with photons with a higher energy than the electron band

gap. Afterwards the electrons will be subject to relaxation, which lowers the energy by vibrational excitation, and subsequently by spontaneous emission emit a photon. The photon emitted has an energy, and thus wavelength, specific to a the characteristic atomic transition.
The photoluminescence spectrum of trivalent ytterbium has been studied before using different host materials. These studies gave us a rough idea as to where were we expect to find photoluminescence as well as the lifetime of the transition. There have been photoluminescence studies of ytterbium in lead phosphate glasses [9], $YAlO_3$ [10], and various other materials [11–14]. These studies all show a peak near 975 nm and a lifetime in the order of 0.7 ms.
Since we cannot control which ion of ytterbium we have in our sample we need to be able to discriminate if whether we see the photoluminescence of divalent or trivalent ytterbium ions since both are stable configurations. From theory we know that the divalent variant of ytterbium has a filled 4f shell. Transitions within the 4f shell are therefore not possible. The only transitions Yb2+ can have are from the 5s or 5p shell to the 6s shell. This transition requires a lot more energy and emits photons in the range of 300 to 500 nm, this has also been confirmed in a number of studies [15]. Which means that there is no problem with differentiating the two different ions.

CHAPTER 2

Methodology

2.1 Sample implantation

We used low pressure chemical vapor deposition to create a 400 nm Si_3N_4 layer on top of 2.5 μm wet oxide on Si wafer. We implanted this layer with ytterbium ions with the same technique used by D.Ding [4]. This technique is based on ionizing the ytterbium atoms and using a magnetic field combined with an aperture to accelerate the ions and select the isotope we are interested in. During implantation the ytterbium ions get stripped of most of their electrons, and gather electrons again when they have come to a rest in the sample. With a Faraday cup the density of implanted ions can be estimated, however this does not give information on the distribution of 2+ and 3+ ions. The samples have been subsequently annealed in nitrogen gas flow, at 1100 °C for 6 hours. Annealing the sample helps reorganize the electrons in the sample making it more likely for trivalent ions to be present. This process also helps restructure the material damage caused by implantation which in theory helps reduce structural damage induced photoluminescence. The samples we implanted have a density of 1e12,1e13 and 1e14 ytterbium particles per cm^2 and we have a sample as implanted and an annealed sample of these densities. A density of 1e14 /cm^2 equates to around 1 in 5000 particles being Yb.

2.2 Setup

2.2.1 Excitation

For the excitation of the Yb3+ ions we mainly used 2 different lasers, a high power 12W 910 nm multi-mode fiber coupled diode laser and a 20 mW scanning single mode fiber coupled laser with a range of 930-980 nm. All measurements shown were done with the use of around 1W 910 nm excitation on the sample. Though the laser we used is has the capability to go to

12W, we can only irradiate the sample with around 1 W of power, since a lot of power is lost using beamsplitters, linear polarizers and the other components in our setup. The laser beam is focused onto the sample using a Olympus 10x microscopy lens with an numerical aperture of 0.25. The linear polarizer we use is set to an angle to only let s-polarized light through. The transmission of the beamsplitter is dependent on the polarization of the incoming light, using s-polarized light we can maximize transmission through the beamsplitter. The polarization of the photoluminescence we assume is random due to vibrational relaxation and since we assume the transition dipole moment direction to be isotropic. The photoluminescence light being randomly polarized means that we can filter out the reflection of the laser with a second linear polarizer. In theory this should be enough to filter the laser light out, in reality polarizers have a limited polarization ratio. This means that we have to use a long pass filter before coupling our signal into the spectrometer.

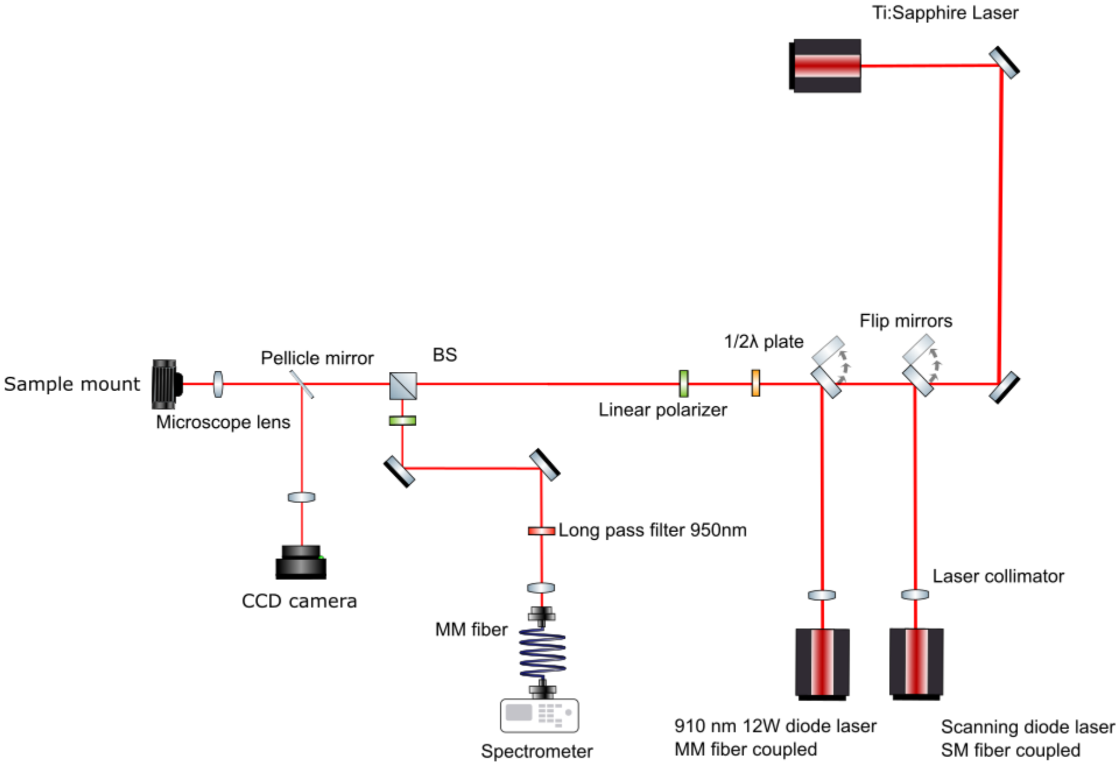

Figure 2.1: *Our experimental setup uses linear polarizers and long pass filters to filter out the laser light. The pellicle mirror combined with the CCD camera is used to align and focus the excitation beam.*

2.2.2 Detection

After being coupled into a multi-mode fiber, the signal gets focused and magnified onto a slit of $100\mu m$. The diameter of the core of the multimode fiber is $104\mu m$. The magnification is equal to $M = \frac{f_2}{f_1} = \frac{100mm}{25mm} = 4.0$. We expect that approximately a quarter of the light travels to the CCD camera as can be seen in figure 2.2. To detect the the photoluminescence from the Yb3+ ions we use a Jobin Yvon Triax-550 spectrometer paired with an Andor iDus 401-series spectroscopy CCD. The data shown in the results was gathered using an exposure time of 20 seconds with a grating setting of 600/mm.

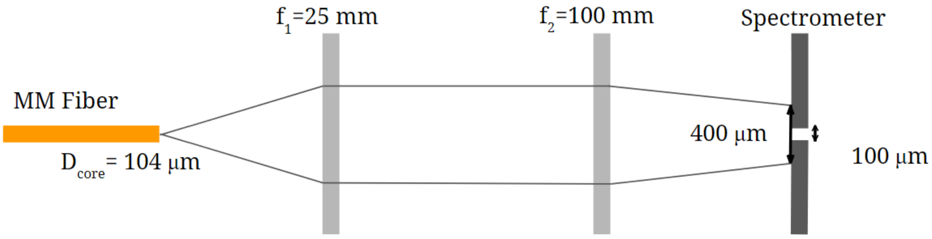

Figure 2.2: *Shown here is the lens configuration and slit of the spectrometer.*

CHAPTER 3

Results and Discussion

3.1 SiN:Yb Spectrum

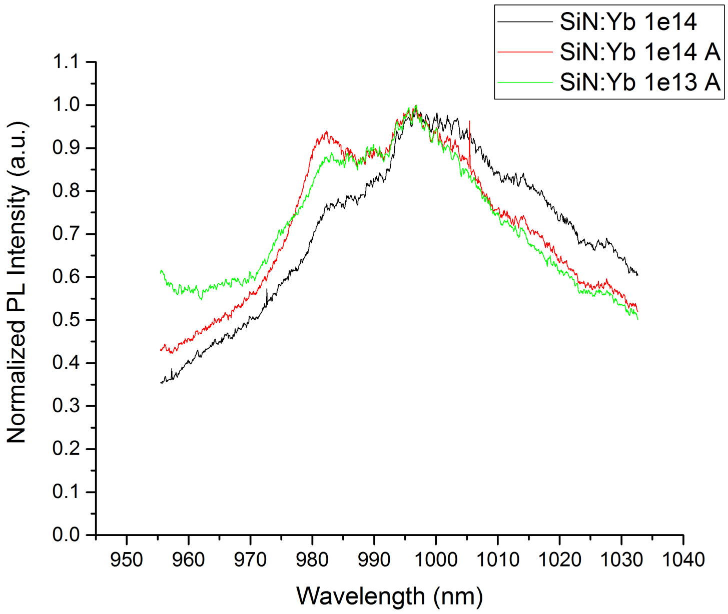

Figure 3.1: *The normalized photoluminescence spectra of three different* Si_3N_4*:Yb samples. Showing both the spectrum of the annealed and as implanted sample with a concentration of 1e14 ions/cm*^{2}*. Additionally we compare it to an annealed sample with a lower Yb density of 1e13 ions/cm*^{2}*.*

3.1.1 Confirming it is Yb3+ fluorescence

How do we know for sure that the 981 nm peak we see is Yb3+ luminescence? This is of course an important question, since the signal is very weak and easily misinterpreted.
The first thing we observed was if the signal we measured was polarization dependent. Since the laser is linearly polarized, we know that any signal that is affected by a polarizer is a result of the laser light. Additionally, the wavelength of this signal is very close to the transition we sought out to find. Lastly, the peak we see at 981 nm is dependent on the density of ytterbium in the sample. These arguments all together make it very unlikely that it would be something else, the only possibility left would be that it a result of implantation damage, however this normally does not a have such a small linewidth.

3.1.2 Fitting of the spectra

We fitted the spectrum of the annealed 1e14 samples with two separate Gaussian curves as can be seen in figures (3.2, 3.3). One wider Gaussian curve fits the background, which has a similar shape. The other smaller Gaussian curve fits the Gaussian peak of the trivalent ytterbium signal. For our fits we used the equation:

$$ae^{\frac{-(x-x_0)^2}{2\sigma_1^2}} + be^{\frac{-(x-x_1)^2}{2\sigma_2^2}}$$

We used the least squares method to find the optimum of the 6 degrees of freedom in this equation.

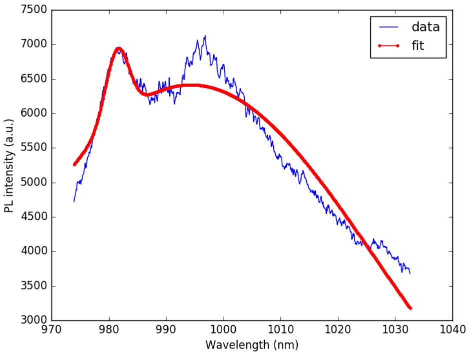

Figure 3.2: *Fit of the photoluminescence spectrum of an annealed 1e14 ions/cm^2 SiN sample. The red curve represents the double Gaussian fit, the blue curve the raw data.*

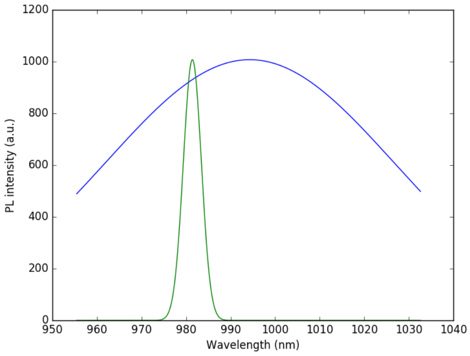

Figure 3.3: *The separate Gaussian curves that were used in the fit of the photoluminescence spectrum to the left.*

3.2 Comparison with Yb in SiO

If we compare the Yb3+ spectrum measured in silicon nitride to the spectrum of Yb3+ in silicon oxide as can be seen in figure 3.4, we see a redshift of around 5 nm. It can already be seen in the large difference in refractive index that the electric susceptibility is higher, we think this difference in environmental potential is responsible for the redshift we observe. Due to the parity forbidden nature of the 4f-4f transition, the energy of this transition is largely sensitive to the environmental potential of the host material, thus small shifts in wavelength are within our realm of expectations. We also observe a background in this spectrum. The origins of this background can be photoluminescence intrinsic to silicon nitride, it can be damage photoluminescence or it could be the other transitions of Yb3+. Other possible explanations to it could be photoluminescence from the silicon wafer, since it has a bandgap at around 1050 nm wich could leak into our spectrum, i.e. there are many possible explanations to the background we see.

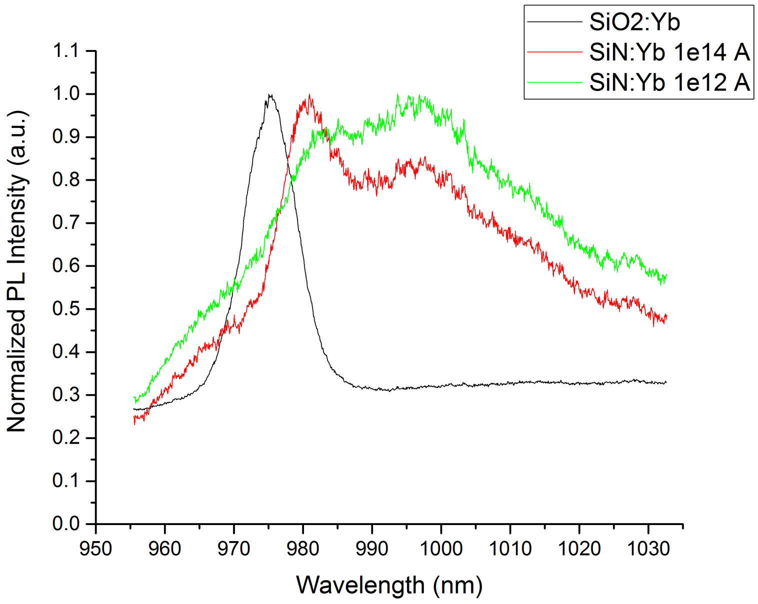

Figure 3.4: *The spectra of two different annealed Si_3N_4 samples with different densities, 1e12 and 1e14 ions/cm^2, green and red respectively. These samples we compare to a SiO_2 calibration sample, in black.*

3.3 Power dependency measurements

By looking at the power dependency we can see whether we saturate the ytterbium ions. In figure 3.5 we see that the intensity of the Yb3+ peak grows linearly with the power, meaning that we do not saturate this transition. However we do see a decrease in growth of the background intensity. This could be an effect of inaccuracy of the fit, but we can also see it in the normalized spectra seen in figure 3.6. At lower power levels the growth of intensity is much larger than that of the Yb3+ peak, but after it reaches the point of 247 mW the normalized spectrum does not change much, which indicates that the whole spectrum increases an equal amount. This would mean that the background does show signs of saturation.

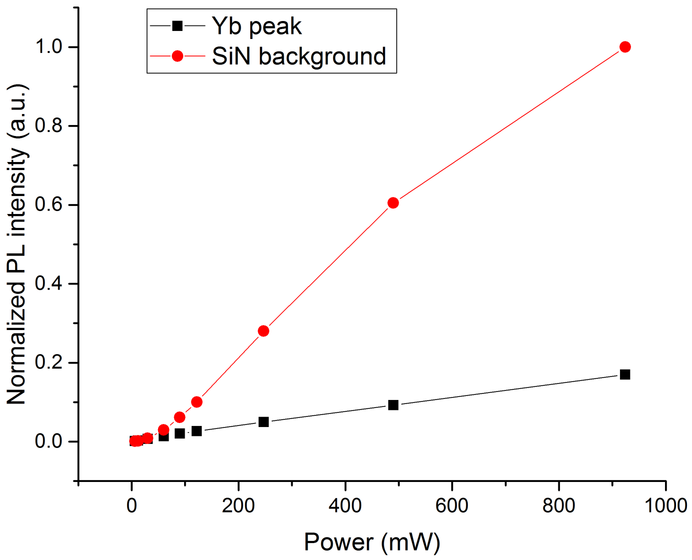

Figure 3.5: The power dependency plot of the annealed 1e14 ions/cm^2 sample. These points represent the height of the fits mentioned in section 3.1.2

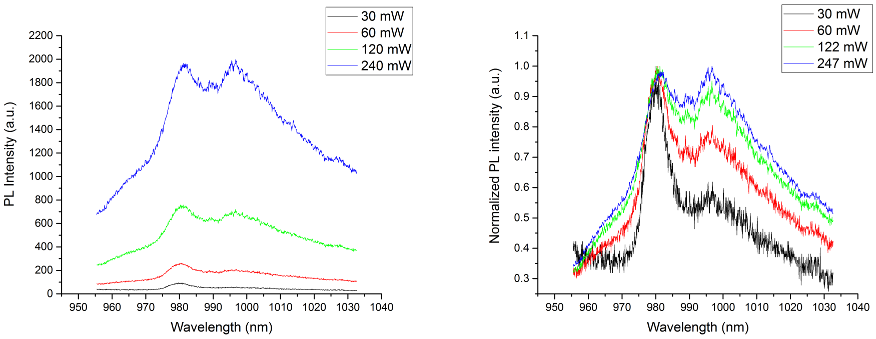

Figure 3.6: *Spectrum of the annealed 1e14 ions/cm^2 sample, at different laser power levels.The graph on the right is a normalized version of the graph on the left, done by dividing by the highest value.*

3.4 Density of Yb3+ ions

To determine how many Yb3+ ions are present in the samples, we first determined the spot size of the laser using the CCD camera. By knowing the area we excite, the number of counts we detect, and the detection efficiency we can calculate how many of the Yb atoms in the sample are trivalent.

3.4.1 Spot size

The spot size was determined by looking at an image of a low power laser spot, taken by the CCD camera as seen in figure 3.7. This image was then analyzed, and we determined the spot size from this. We first created a boolean array out of the image and then fitted a circle to this image, as can be seen in figure and 3.8. The fitting algorithm gave us an idea of the radius, and thus the area of this circle. Calculating the detection area and excitation area gave us $A_{det} = 173\mu m^2$ and $A_{exc} = 678\mu m^2$.

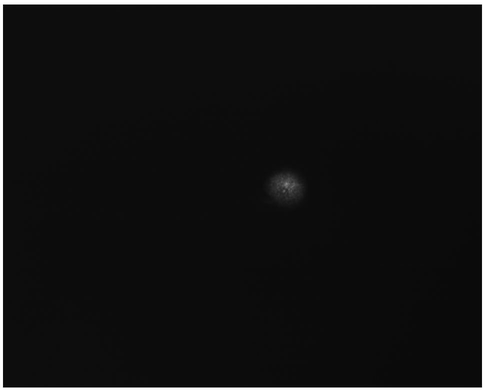

Figure 3.7: Image of the laser spot taken by the CCD camera.

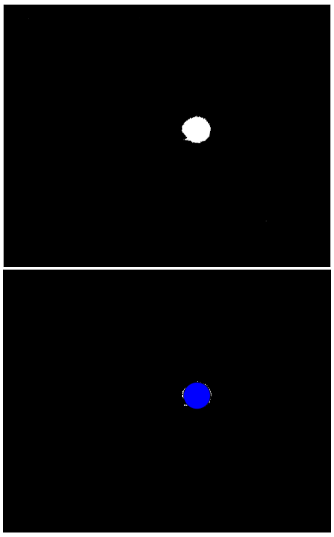

Figure 3.8: Boolean image and the circle fit of the image to the left.

3.4.2 Detection efficiency

As mentioned in the methodology we capture the photoluminescence emitted by Yb3+ we use microscopy lens with an numerical aperture of 0.25 according to figure 2.2, this means that only 5.2% of the photons emitted in our detection area is captured. The light emitted then goes through a beamsplitter which means only half of the signal goes through, it subsequently travels through a linear polarizer which would reduce the signal by half as well. This means when factoring all of these effects in that only 1.3% of all photons from Yb3+ photoluminescence reach the spectrometer.

To measure the detection efficiency of the CCD camera, we had to use a very low power laser signal since the detector would otherwise be damaged. To achieve this we used the laser on a low power setting but high enough to measure with the power meter which is in the order of μW , and we used neutral density filters to use for the detection. The laser is set to a wavelength near to where we found the 980 nm peak. We then were able to equate the power of the signal to a number of photons we can detect. Since the peak we measure has a certain linewidth, we cannot simply take the maximum of this peak to get the number of counts. We have to integrate over the width of the peak to find the total number of counts in the peak. Using this method gave us a rough indication of how many photons fall onto the detector per count, which in our case was $\approx$ 1508 photons/count.

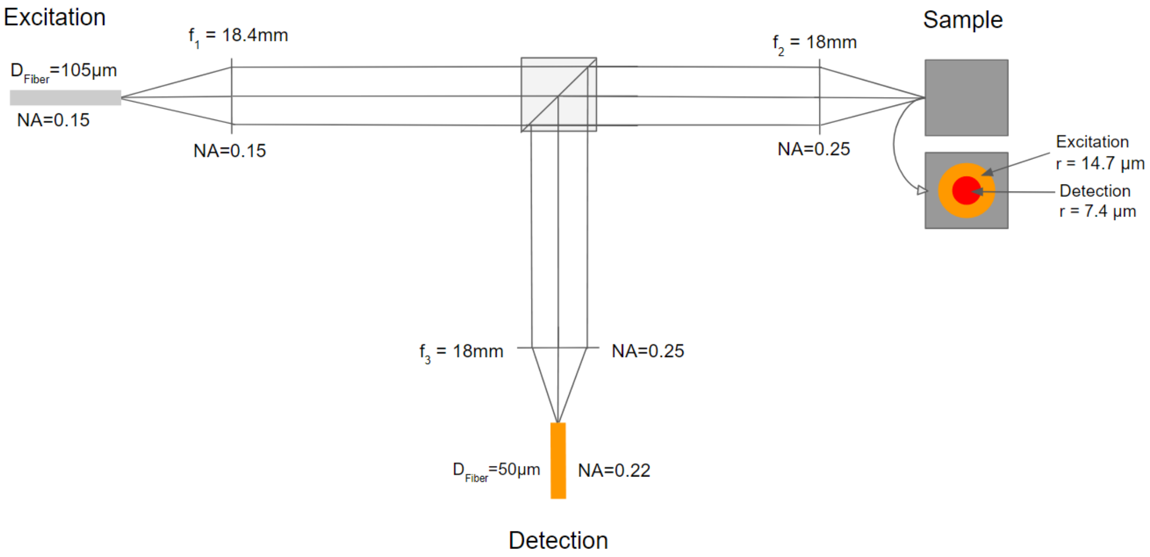

Figure 3.9: *A simplified version of our setup before our signal goes into the spectrometer. This gives us an insight into the efficiency of our detection.*

3.4.3 Estimation of Yb3+ density

We estimate the total number of Yb3+ that we were able to excite, and emitted a photon corresponding to the 4f-4f transition of 980 nm by using the ratio of 1508 photons/count we found in the previous section. We also use the same integration method mentioned to calculate the number of counts found in the 980 nm peak in our spectrum. However the background first has to be subtracted from this peak using the fits mentioned in section 3.1.2. This gave us the number of counts given by the 980 nm Yb3+ peak, which was around 6E4 counts with an exposure time of 20 s. using the efficiency mentioned before we can calculate the number of detected photons per second, $n_{det} = \frac{6\times10^4 \cdot 1508}{20s} \approx 1.36 \times 10^7 s^{-1}$. We know this is 1.3 % of emitted photons. Thus the total amount of photons emitted per second by Yb3+ would be equal to $n_{total} = 1.36 \times 10^7 s^{-1}/0.013 \approx 1.05 \times 10^9 s^{-1}$. Using the lifetime we found in other studies mentioned in 1.2.2 we can estimate the number of Yb3+ ions that emitted a photon, $n_{total} \cdot \tau_{Yb} = 1.05 \times 10^9 s^{-1} \cdot 0.7 \times 10^{-3} s = 7.32 \times 10^5 = N_{total}$. With the total amount of Yb3+ ions excited, the density of Yb particles and the area of detection we can calculate the density of excited Yb3+ ions and what fraction of Yb particles it is. Calcultating the density gives us $\rho_{Yb3+} = N_{total}/A_{det} = 7.32 \times 10^5/1.73 \times 10^{-7} cm^2 = 4.23 \times 10^{12} cm^{-2}$, this is within two orders of the implanted dose which we think is a realistic estimation.

CHAPTER 4

Conclusion

One of our main results is that we were able to measure the spectrum of Yb3+ in silicon nitride, this already gave us some insight into the spectroscopic properties that this material has. One of these insights is the fact that it is essential to anneal the samples to find any semblance of the characteristic Yb3+ peak. Thus we could say that too little Yb3+ is formed after implantation to be able to see photoluminescence. In samples with an implantation density lower than 1e14 ions/cm^2 there is also too little Yb3+ formed, even after annealing.

Another observation we made was that the peak we measured seemed to be redshifted by around 5 nm. An explanation for this could be the fact that the host material disturbs the electrons in such a way that the transition of 980 nm is more allowed than the transition of 976 nm. Moreover, silicon nitride with respect to silicon oxide is more dense and has a higher refractive index, these properties could result in difference in wavelength as also observed by D.C.Yeh et al. [12]

It also shows in figure 3.1 that the spectra we measured have very noticeable background. Though the origins of this background is uncertain, we do have some thoughts on this. The power dependency plots seen in figure 3.5 show that the intensity of the background increases faster than that of the 980 nm peak. This we perceive as there being a higher density of states of this background than that of the Yb3+ transition, this would indicate that the background is not caused by other Yb3+ transitions. Though what also might have an effect is the self trapping of the 980 nm Yb3+ transition, since the absorption and excitation overlap at that point, this was also an observation by K.Venkata et al. [9]. Additionally, the intensity of the background see,s to be inversely proportional to the density of Yb particles, the chance of this background to be different Yb3+ transitions is thus slim.

4.1 Outlook

A continuation of this research would be to investigate more spectroscopic properties of ytterbium in silicon nitride, for instance the fluorescence lifetime. This could also tell us more about the origins of background in the spectrum, the Yb3+ transition has a long lifetime making it easy to distinguish. An option for an experiment would be to use a continuous wave source and a optical chopper. Pulsed laser source could also be used to achieve this.

A problem that has yet to be solved is saturation of the Yb3+ transition. But achieving this would be very hard since more power would have a chance of damaging the samples. The same damage considerations hold for stronger focusing.

A higher density of Yb can also help understand the properties of SiN:Yb as well as different annealing processes. The annealed 1e14 ions/cm^2 is the only sample where we were certain to have found the Yb3+, in the future we are interested in comparing this with higher densities. Additionally, what misses is a reference sample without any ytterbium in it. Measuring a sample without any ytterbium would help in determining if the background is intrinsic to amorphous silicon nitride, if it is photoluminescence caused by implantation damage, or if other ytterbium transitions lie at the root of this.

A measurement using waveguides is also an option for the future. Using waveguides would increase the chance of the ytterbium to become excited. This works by etching the silicon nitride away from the sample leaving only silicon oxide, in such a manner that only a strip of silicon nitride is left. This strip can then be used as waveguide when irradiated from the side. This could amplify the photoluminescence dependent on the length.

Lastly the final goal was the production of ytterbium doped silicon nitride microresonators. We are able to draw the conclusion that a density of 1e13/cm^2 ions or lower is less than ideal. Thus microresonators would have to be made out of annealed samples of at least 1e14/cm^2 ytterbium ions. Our finding of SiN:Yb3+ PL here suggests that this is a useful next step.

4.2 Acknowledgements

I would like to use this section to show my gratitude to everyone that has helped me make this bachelor research project possible. First of all I would like to thank my daily supervisor Wolfgang Löffler for providing me with excellent advise, useful information and help during the course of the project. I would like to thank Dirk Bouwmeester for giving me the opportunity to work on this project in the quantum optics group. In addition, I would like to show my gratitude to the quantum optics group as a whole for providing an great setting to work in and for the many occasions of celebratory cake. Lastly I would like to thank Tim Fuchs as well as Thom Boudewijn, Jessamy Mol and Iraitz Gorroño for providing valuable discussion and some distraction at times this was needed.

References

[1] M. Afzelius, N. Gisin, and H. De Riedmatten, *Quantum memory for photons*, Physics Today **68**, 42 (2015).

[2] P. Siyushev, K. Xia, R. Reuter, M. Jamali, N. Zhao, N. Yang, C. Duan, N. Kukharchyk, A. D. Wieck, R. Kolesov, and J. Wrachtrup, *Coherent properties of single rare-earth spin qubits*, Nature Communications **5**, 1 (2014).

[3] D. Ding, M. J. a. de Dood, J. F. Bauters, M. J. R. Heck, J. E. Bowers, and D. Bouwmeester, *Fano resonances in a multimode waveguide coupled to a high-Q silicon nitride ring resonator*, Optics Express **22**, 6778 (2014).

[4] D. Ding, L. M. C. Pereira, J. F. Bauters, M. J. R. Heck, G. Welker, A. Vantomme, J. E. Bowers, M. J. A. de Dood, and D. Bouwmeester, *Multidimensional Purcell effect in an ytterbium-doped ring resonator*, Nature Photonics **10**, 385 (2016).

[5] Y. Gong, M. Makarova, S. Yerci, R. Li, M. J. Stevens, B. Baek, S. W. Nam, R. H. Hadfield, S. N. Dorenbos, V. Zwiller, J. Vuckovic, and L. Dal Negro, *Linewidth narrowing and Purcell enhancement in photonic crystal cavities on an Er-doped silicon nitride platform.*, Optics express **18**, 2601 (2010).

[6] G. C. Righini, Y. Dumeige, P. Féron, M. Ferrari, G. N. Conti, D. Ristic, and S. Soria, *Whispering Gallery Mode microresonators: Fundamentals and applications*, Rivista del Nuovo Cimento **34**, 435 (2011).

[7] W. A. Phillips, *Tunneling states in amorphous solids*, Journal of Low Temperature Physics **7**, 351 (1972).

[8] A. Fleischmann and C. Enss, *Geheimnis der Tunnelsysteme*, Physic Journal **6**, 41 (2007).

[9] K. Venkata Krishnaiah, R. Rajeswari, K. Upendra Kumar, S. Surendra Babu, I. R. Mart??n, and C. K. Jayasankar, *Spectroscopy and radiation trapping of Yb3+ ions in lead phosphate glasses*, Journal of Quantitative Spectroscopy and Radiative Transfer **140**, 37 (2014).

[10] M. J. Weber, *Optical Properties of Yb3+ and Nd3+ - Yb3+ Energy Transfer in YAlO3*, Physical Review B **4**, 3153 (1971).

[11] G. Boulon, A. Brenier, L. Laversenne, Y. Guyot, C. Goutaudier, M. T. Cohen-Adad, G. E. Métrat, and N. Muhlstein, *Search of optimized trivalent ytterbium doped-inorganic crystals for laser applications,* Journal of Alloys and Compounds **341**, 2 (2002).

[12] D. Yeh and W. Sibley, *RADIATION EFFECTS AND OPTICAL IN Yb DOPED BARIUM-THORIUM,* Journal of Non-Crystalline Solids , 66 (1986).

[13] N. V. Kuleshov, a. a. Lagatsky, V. G. Shcherbitsky, V. P. Mikhailov, E. Heumann, T. Jensen, A. Diening, and G. Huber, *CW laser performance of Yb and Er,Yb doped tungstates,* Applied Physics B: Lasers and Optics **64**, 409 (1997).

[14] C. Strohhöfer and A. Polman, *Absorption and emission spectroscopy in Er3+,Yb3+ doped aluminum oxide waveguides,* Optical Materials **21**, 705 (2003).

[15] V. I. Solomonov, V. V. Osipov, and A. V. Spirina, *Luminescence and absorption of divalent ytterbium ion in yttrium-aluminum garnet ceramics,* Optics and Spectroscopy **117**, 441 (2014).